Star Formation Main Sequence in a Hierarchical Universe

ChangHoon Hahn[1], **Jeremy L. Tinker**[2], **Andrew R. Wetzel**[3,4,5]

changhoon.hahn@lbl.gov

DRAFT --- 258e9ee --- 2018-01-12 --- NOT READY FOR DISTRIBUTION

ABSTRACT

motivation, methodology, impact. In observations star forming galaxies form a tight $log\ M_*$ to $log\ SFR$ relation referred to as the *star formation main sequence* (SFMS) out to $z \sim 2$. Beyond the evolution "along" this SFMS, however, the star formation histories of star forming galaxies have not been precisely characterized. The SFH of these galaxies govern SMF, SFMS, and also observed constraints on the stellar mass to halo mass relation.

By combining high-resolution cosmological N-body simulation with observed evolutionary trends of SF galaxies, we construct a model that tracks the evolution of star forming central galaxies over the redshift $z < 1$. Comparing this model

Observations find a remarkably small scatter in the stellar mass to halo mass relation. Somehow the star formation histories of galaxies must

According to observations, star forming galaxies form a tight $log\ M_*$ to $log\ SFR$ relation referred to as the "star formation main sequence" out to $z \sim 2$.

Subject headings: **methods: numerical – galaxies: clusters: general – galaxies: groups: general – galaxies: evolution – galaxies: haloes – galaxies: star formation – cosmology: observations.**

Checklist

- Check the correlation between halo growth rate with different t_{delay} and δt_{abias} with the total halo growth rate between $z \sim 0$ and $z \sim 1$.

[1]Lawrence Berkeley National Laboratory, 1 Cyclotron Road, Berkeley, CA 94720

[2]Center for Cosmology and Particle Physics, Department of Physics, New York University, 4 Washington Place, New York, NY 10003

[3]TAPIR, California Institute of Technology, Pasadena, CA USA

[4]Carnegie Observatories, Pasadena, CA USA

[5]Department of Physics, University of California, Davis, CA USA

1. Introduction

- Motivate why we think SF galaxies evolve along the main sequence
- Discuss the current thought process on galaxy assembly bias
- Explain the limitation of SFH derivable from observations (Claire's fisher matrix paper would be really good; ask her about the details)
- Observations also can't provide detail host dark matter halo properties
- So the approach with combining observations with N-body (empirical modeling) is very effective in the context of the halo.
- Maybe talk about how the bigger context of why this is important?
- Why only centrals – because our current best understanding of satellites is that they quench after infall, so it doesn't make sense to look at them

2. Central Galaxies of SDSS DR7

We construct our galaxy sample following the sample selection of Tinker et al. (2011). We select a volume-limited sample of galaxies with $M_r 5 log(h) < 18$ and complete in $M_* > 10^{9.4} M_\odot$ from the NYU Value-Added Galaxy Catalog (VAGC; Blanton et al. 2005) of the Sloan Digital Sky Survey Data Release 7 (SDSS DR7; Abazajian et al. 2009) at $z \approx 0.04$. The stellar masses of these galaxies are estimated using the `kcorrect` code (Blanton & Roweis 2007) assuming a Chabrier (2003) initial mass function. The star formation of the galaxies are estimated spectroscopically using the specific star formation rates (SSFR) from the current release of the MPA-JHU spectral reductions[1] (Brinchmann et al. 2004). Generally speaking, SSFR $> 10^{-11}\mathrm{yr}^{-1}$ are derived from H_α emission, $10^{-11} >$ SSFR $> 10^{-12}\mathrm{yr}^{-1}$ are derived from a combination of emission lines, and SSFR $< 10^{-12}\mathrm{yr}^{-1}$ are based on D_n4000 (see discussion in Wetzel et al. 2013). We note that SSFR $< 10^{-12}\mathrm{yr}^{-1}$ should only be considered upper limits to the true galaxy SSFR (Salim et al. 2007).

From our galaxy sample, we identify the central galaxies using the Tinker et al. (2011) halo-based group-finding algorithm, which is based on the Yang et al. (2005) algorithm and tested in Campbell et al. (2015). The algorithm assigns a probability of being a satellite, P_{sat}, to each galaxy in the sample. Galaxies with $P_{\mathrm{sat}} \geq 0.5$ are classified as satellites and $P_{\mathrm{sat}} < 0.5$ are classified as centrals. In this paper we focus on central galaxies. With any group finding algorithm, galaxies are misassigned due to projection effects and redshift space

[1] http://wwwmpa.mpa-garching.mpg.de/SDSS/DR7/

distortions. The purity of the full central galaxy sample is $\sim 90\%$ with a completeness of $\sim 95\%$ (Tinker et al. 2017). Furthermore, Campbell et al. (2015) find that the algorithm robustly identifies red and blue centrals as a function of stellar mass, which is highly relevant to our analysis.

In the left panel of Figure 1, we plot the SFR-M_* distribution of the SDSS DR7 central galaxies. In the right panel, we plot the distribution of SSFR, $p(\log \mathrm{SSFR})$, for galaxies with $10.6 < \log M_* < 10.8$ (stellar mass range highlighted on the left panel). Both panels of Figure 1 illustrate the bimodality in the galaxy sample. The SFR-M_* distribution also illustrate the correlation between SFR and M_* in star-forming galaxies *i.e.* the star-formation main sequence (SFMS).

3. Model: Simulated Central Galaxies

We're interesting in constructing a model that tracks central galaxies and their star formation within the heirarchical growth of their host halos. This requires a cosmological N-body simulation that accounts for the complex dynamical processes that govern the host halos of galaxies. In this paper we use the high resolution N-body simulation from Wetzel et al. (2013) generated using the White (2002) `TreePM` code with flat ΛCDM cosmology ($\Omega_m = 0.274, \Omega_b = 0.0457, h = 0.7, n = 0.95, \mathrm{and} \sigma_8 = 0.8$). From initial conditions at $z = 150$ generated from second-order Lagrangian Perturbation Theory, 2048^3 particles with mass of $1.98 \times 10^8\,M_\odot$ are evolved in a 250Mpc/h box with a Plummer equivalent smoothing of $2.5\,\mathrm{kpc}/h$. For a more detailed description of the simulation, we refer readers to Wetzel et al. (2013, 2014).

From the TreePM N-body simulation, 'host halos' are identified using the Friends-of-Friends (FoF) algorithm of Davis et al. (1985) with linking length of $b = 0.168$ times the mean inter-partcile spacing. Within these host halos, Wetzel et al. (2013) identifies 'subhalos' as overdensities in phase space through a six-dimensional FoF algorithm (FoF6D White et al. 2010). The host halos and subhalos are then tracked across the 45 simulation outputs from $z = 10$ to 0 to build merger trees (Wetzel et al. 2009; Wetzel & White 2010). The most massive subhalos in newly-formed host halos at a given simulation output are defined as the 'central' subhalo. A central subhalo retains its 'central' definition until it falls into a more massive host halo, at which point it becomes a 'satellite' subhalo.

Each subhalo is assigned a M_peak, the maxmum host halo mass that it ever had as a central subhalo. Using M_peak, we construct a galaxy catalog from the subhalos using subhalo abundance matching (SHAM; Vale & Ostriker 2006; Yang et al. 2009; Wetzel et al. 2012, 2013, 2014; Hahn et al. 2017)**citations conroy2006, leja2013**. In principle, SHAM assumes a one-to-one mapping between subhalo M_peak and galaxy stellar mass M_*: $n(> M_\mathrm{peak}) > n(> M_*)$ that preserves the rank ordering. In practice, we apply a 0.2 dex log-normal scatter in M at fixed M_peak based on observations of the stellar mass to halo mass relation (SMHMR;

bunch of SMHMR citations). Gu et al. (2016) compile empirical constraints on the scatter of this stellar mass to halo mass relation ($\sigma_{\log M_*}$). Using the SHAM mapping, we can assign galaxy stellar mass to subhalos based on observed stellar mass functions (SMFs) at the redshifts of the simulation outputs (snapshots). By assigning galaxy M_* independently at each snapshot, we not only track the evolution of subhalos, but also the evolution of the galaxies' M_*.

In our SHAM prescription, we use the SMF from Li & White (2009) at $z = 0.05$ and interpolate at higher redshifts between the Li & White (2009) SMF and the SMF from Marchesini et al. (2009) at $z = 1.6$. We choose the Li & White (2009) SMF because it is based on the same SDSS NYU-VAGC sample as our SDSS DR7 group catalog (see Section 2). We choose the Marchesini et al. (2009) SMF, amongst others, because it produces interpolated SMFs that monotonically increase at $z < 1$. As noted in **?**, at $z \approx 1$, the SMF interpolated between the Li & White (2009) and Marchesini et al. (2009) SMFs is consistent with more recent measurements from Muzzin et al. (2013) and Ilbert et al. (2013). As we describe later in this section, we are only interested in the snapshots at $z \approx 0.05$ and 1.

3.1. Selecting $z \sim 0$ Star Forming Central Galaxies

In order to examine the evolution of star-forming central galaxies, we require a model that tracks **finish**. To construct this model, we first select star-forming galaxies from the central galaxies in our simulation (Section 3). Since we're ultimately interested in comparing our model to observation, our selection is based on $f^{\rm cen}_{\rm SFMS}(M_*)$, the fraction of central galaxies within the star-forming main sequence, measured from the SDSS DR7 VAGC (Section 2). Below, we describe how we derive this $f^{\rm cen}_{\rm SFMS}(M_*)$.

When classifying galaxies, often in the literature, an empirical color-color or SFR-M_* cut that separates the two main modes (red/blue or star-forming/quiescent) in the distribution is chosen (**Baldry et al. 2006; Drory et al. 2009; Cooper et al. 2010; Iovino et al. 2010; Peng et al. 2010; Geha et al. 2012; Kovac et al. 2014; Hahn et al. 2015., moustakas2012,hahn2015**). The red/quiescent or blue/star-forming fractions derived from this sort of classification by construction depend on the choice of cut and neglect the transitioning galaxies *i.e.* the galaxies in the "green valley". For our $f^{\rm cen}_{\rm SFMS}(M_*)$ measurement, we instead use a method based on the SFMS fitting method from Tjitske et al. (in prep).

The SFMS fitting scheme first divides our SDSS DR7 VAGC central galaxy sample (Section 2) into stellar mass bins of width $\Delta \log M_* = 0.2$ dex. We then fit the SSFR distribution of each stellar mass bin using Gaussian mixture models (GMMs) with $1 - 3$ components using the expectation-maximization algorithm (EM; Dempster et al. 1977; Neal & Hinton 1998). We restrict the models to a maximum of 3 components to account for the three possible galaxy classifications: quiescent, star-forming, and green valley populations. Among the

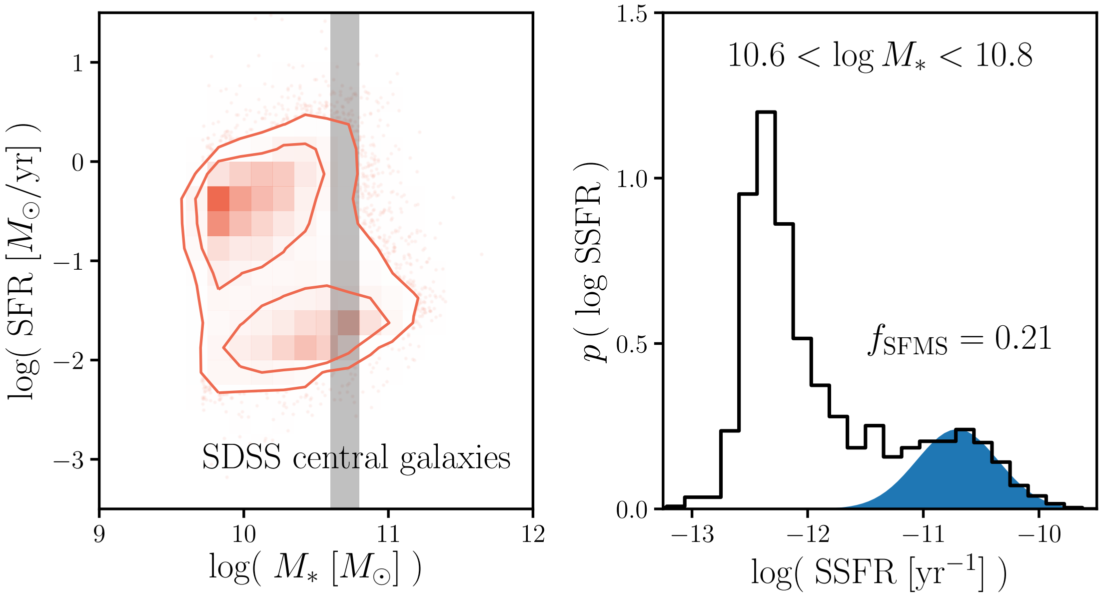

Fig. 1.— SDSS DR7 Group Catalog. Fitting of the SFMS.

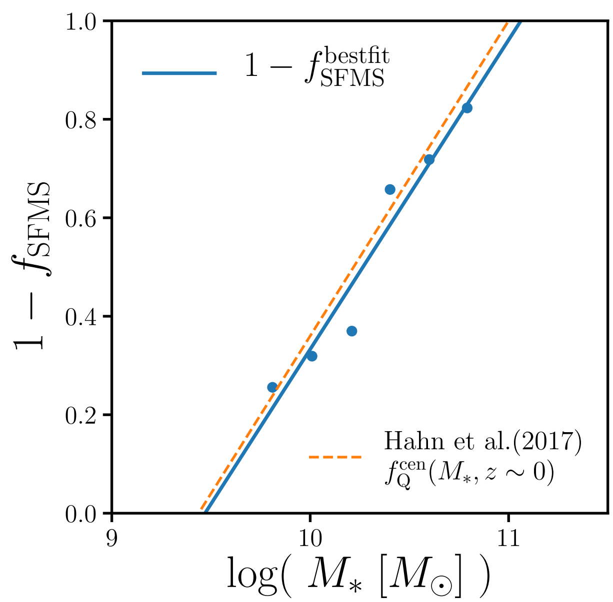

Fig. 2.— SFMS fraction versus quiescent fraction from Hahn

GMMs, the model with the lowest Bayesian Information Criteria (BIC Schwarz 1978) is selected. The Gaussian component of this GMM with mean $\log \mathrm{SSFR} > -11$ represents the SFMS. In the rare cases when more than one GMM component has mean $\log \mathrm{SSFR} > -11$, we compare the weights of the components. If the weight of one component is less than a third of the other, we take the component with the higher weight to represent the SFMS; otherwise, we omit the stellar mass bin altogether. The weight of the SFMS GMM component provides an estimate of $f^{\mathrm{cen}}_{\mathrm{SFMS}}$ for the stellar mass bin.

In the right panel of Figure 1, we plot the SFMS GMM component (blue shaded region) of the $p(\log \mathrm{SSFR})$ for the SDSS DR7 central galaxies within $10.6 < \log M_* < 10.8$. The SFMS constitutes $f^{\mathrm{cen}}_{\mathrm{SFMS}} = 0.21$ of the SDSS central galaxies in this stellar mass bin. Next, using $f^{\mathrm{cen}}_{\mathrm{SFMS}}$ spanning the different stellar mass bins, we fit $f^{\mathrm{cen}}_{\mathrm{SFMS}}$ as a function of M_*. Using a fiducial stellar mass of $\log M_{\mathrm{fid}} = 10.5$, we derive the following best-fit

$$f^{\mathrm{cen}}_{\mathrm{SFMS,bestfit}}(M_*) = -0.627\,(\log M_* - 10.5) + 0.354. \tag{1}$$

In Figure 2, we compare $1 - f^{\mathrm{cen}}_{\mathrm{SFMS}}(M_*)$ (blue scatter) to $f^{\mathrm{cen}}_{\mathrm{Q}}(M_*; z \sim 0)$ from Hahn et al. (2017).

- Then explain how it's not circular because the integrated M_* has to reproduce the same SMF

3.2. Evolving along the Main Sequence

- Talk about the SFR and M_* prescriptions
- parameterization of SFMS
- explicitly talk about the free parameters of the model.
- priors for β_M and β_z encompass the observable constraints
- talk about inference using ABC

4. Results

4.1. The duty cycle of star formation

- Figure that illustrates the fit to observables
- Figure of sigma M star as a function of duty cycle compared to observations

4.2. The need for a galaxy assembly bias

- discuss how t_{duty} is not enough to be consistent with σ_{M_*}.
- first clarify what you mean by galaxy assembly bias
- discuss implementation of galaxy assembly bias
- Figure (pedagogical) of dlogSFR versus dMh dt for different correlation amounts
- Figure of different tdelay and dtabias
- Figure of sigma M star as a function of duty cycle and realistic dt abias and t delay

5. Discussion

5.1. Rethinking the Main Sequence?

- Test the SMHMR for Louis's SFHs

6. Summary

A. $z \sim 1$ observations

Much of the results presented in this paper are based on comparison between our model and observations at $z \sim 0$.. Our model is initalized at $z \sim 1$. Therefore, in this section we test some of the choices we make in our intializations.

- Test impact of $z \sim 1$ SMF
- Test impact of $z \sim 1$ $\sigma_{\log M_*}$

Acknowledgements

Louis Abramson

REFERENCES

Abazajian, K. N., Adelman-McCarthy, J. K., Agüeros, M. A., et al. 2009, The Astrophysical Journal Supplement Series, 182, 543

Blanton, M. R., & Roweis, S. 2007, The Astronomical Journal, 133, 734

Blanton, M. R., Schlegel, D. J., Strauss, M. A., et al. 2005, The Astronomical Journal, 129, 2562

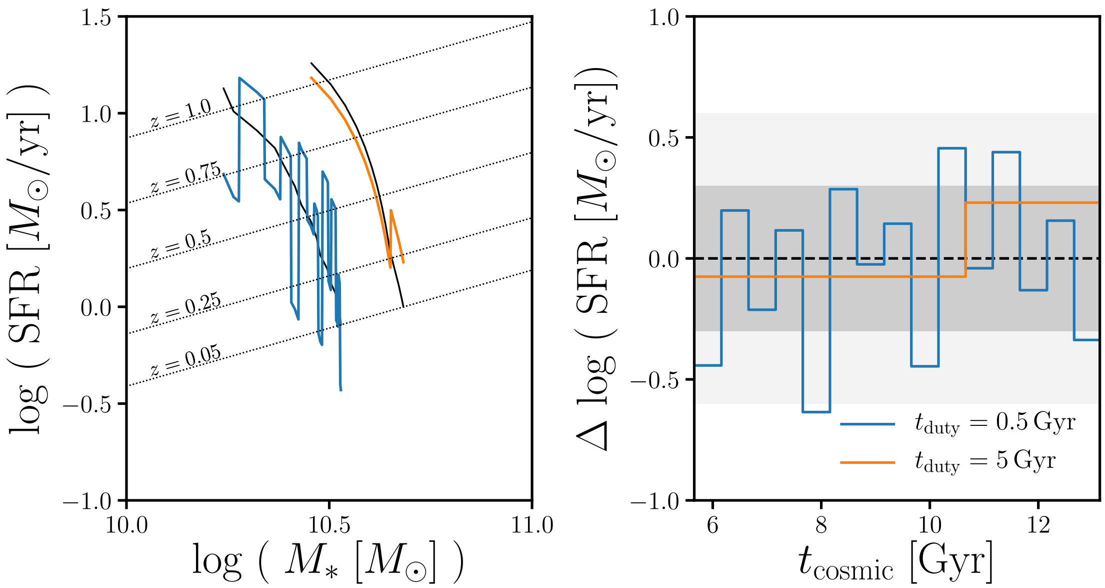

Fig. 3.— Pedagogical figure that illustrates how star forming central galaxies in our model evolve along the SFMS.

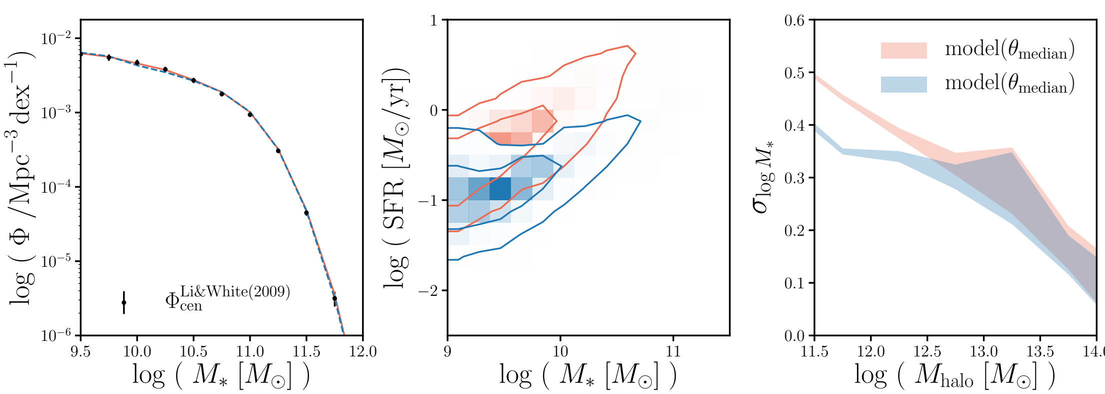

Fig. 4.—

Brinchmann, J., Charlot, S., White, S. D. M., et al. 2004, Monthly Notices of the Royal Astronomical Society, 351, 1151

Campbell, D., van den Bosch, F. C., Hearin, A., et al. 2015, Monthly Notices of the Royal Astronomical Society, 452, 444

Chabrier, G. 2003, Publications of the Astronomical Society of the Pacific, 115, 763

Davis, M., Efstathiou, G., Frenk, C. S., & White, S. D. M. 1985, The Astrophysical Journal, 292, 371

Dempster, A. P., Laird, N. M., & Rubin, D. B. 1977, Journal of the Royal Statistical Society. Series B (Methodological), 39, 1

Gu, M., Conroy, C., & Behroozi, P. 2016, The Astrophysical Journal, 833, 2

Hahn, C., Tinker, J. L., & Wetzel, A. R. 2017, The Astrophysical Journal, 841, 6

Ilbert, O., McCracken, H. J., Le Fèvre, O., et al. 2013, Astronomy and Astrophysics, 556, A55

Li, C., & White, S. D. M. 2009, Monthly Notices of the Royal Astronomical Society, 398, 2177

Marchesini, D., van Dokkum, P. G., Förster Schreiber, N. M., et al. 2009, The Astrophysical Journal, 701, 1765

Muzzin, A., Marchesini, D., Stefanon, M., et al. 2013, The Astrophysical Journal, 777, 18

Neal, R. M., & Hinton, G. E. 1998, in Learning in Graphical Models, NATO ASI Series (Springer, Dordrecht), 355

Salim, S., Rich, R. M., Charlot, S., et al. 2007, The Astrophysical Journal Supplement Series, 173, 267

Schwarz, G. 1978, The Annals of Statistics, 6, 461

Tinker, J., Wetzel, A., & Conroy, C. 2011, ArXiv e-prints, 1107, arXiv:1107.5046

Tinker, J. L., Hahn, C., Mao, Y.-Y., & Wetzel, A. R. 2017, arXiv:1705.08458 [astro-ph], arXiv:1705.08458 [astro-ph]

Vale, A., & Ostriker, J. P. 2006, Monthly Notices of the Royal Astronomical Society, 371, 1173

Wetzel, A. R., Cohn, J. D., & White, M. 2009, Monthly Notices of the Royal Astronomical Society, 395, 1376

Wetzel, A. R., Tinker, J. L., & Conroy, C. 2012, Monthly Notices of the Royal Astronomical Society, 424, 232

Wetzel, A. R., Tinker, J. L., Conroy, C., & van den Bosch, F. C. 2013, Monthly Notices of the Royal Astronomical Society, 432, 336

—. 2014, Monthly Notices of the Royal Astronomical Society, 439, 2687

Wetzel, A. R., & White, M. 2010, Monthly Notices of the Royal Astronomical Society, 403, 1072

White, M. 2002, The Astrophysical Journal Supplement Series, 143, 241

White, M., Cohn, J. D., & Smit, R. 2010, Monthly Notices of the Royal Astronomical Society, 408, 1818

Yang, X., Mo, H. J., & van den Bosch, F. C. 2009, The Astrophysical Journal, 695, 900

Yang, X., Mo, H. J., van den Bosch, F. C., & Jing, Y. P. 2005, Monthly Notices of the Royal Astronomical Society, 356, 1293

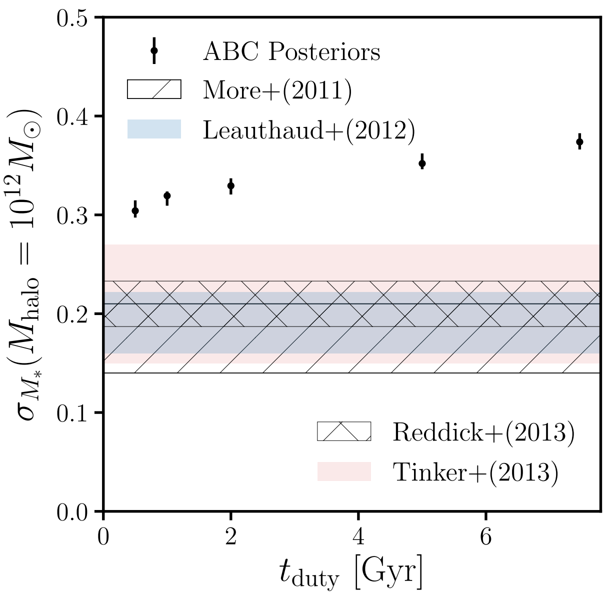
ABC Posteriors
More+(2011)
Leauthaud+(2012)
Reddick+(2013)
Tinker+(2013)
$\sigma_{M_*}(M_{\rm halo} = 10^{12} M_\odot)$
$t_{\rm duty}$ [Gyr]
0.0
0.1
0.2
0.3
0.4
0.5
0
2
4
6

Fig. 5.—